The American Journal of Pathology, Vol. 180, No. 3, March 2012
Copyright © 2012 American Society for Investigative Pathology.
Published by Elsevier Inc. All rights reserved.
DOI: 10.1016/j.ajpath.2011.11.033

Cell Injury, Repair, Aging and Apoptosis

Cathepsin Cleavage of Sirtuin 1 in Endothelial Progenitor Cells Mediates Stress-Induced Premature Senescence

Jun Chen,* Sandhya Xavier,* Eliza Moskowitz-Kassai,* Robert Chen,* Connie Y. Lu,* Kyle Sanduski,* Aleš Špes,* Boris Turk,[†‡] and Michael S. Goligorsky*

From the Departments of Medicine, Pharmacology, and Physiology, Renal Research Institute, New York Medical College, Valhalla, New York; the Department of Biochemistry and Molecular and Structural Biology,[†] Jozef Stefan Institute, Ljubljana, Slovenia; and the Center of Excellence for Integrated Approaches in Chemistry and Biology of Proteins,[‡] Ljubljana, Slovenia*

Stress-induced premature senescence (SIPS) of endothelial cells (ECs) has emerged as a contributor to global EC dysfunction. One of the cellular abnormalities mechanistically linked to SIPS is lysosomal dysfunction. In this study, we examined the impact of a range of cardiovascular risk factors on the expression of sirtuin 1 (SIRT1), SIPS, and apoptosis, and we documented the role of SIRT1 in reduced EC and endothelial progenitor cell (EPC) viability. These findings were confirmed in mice with selective endothelial SIRT1 knockout. The effects of stressors could be partially mimicked by inducing lysosomal membrane permeabilization or inhibiting autophagy, and were reversed by a cathepsin inhibitor. We provide evidence that SIRT1 is an important substrate of cysteine cathepsins B, S, and L. An antioxidant/peroxynitrite scavenger, ebselen, prevented stress-induced SIRT1 depletion and subversion of autophagy by mitigating lysosomal dysfunction. In conclusion, our data advance the concept of "stem cell aging" by establishing the critical role of lysosomal dysfunction in the development of SIPS through the cathepsin-induced proteolytic cleavage of SIRT1, a mechanism linking cell stress to apoptosis and SIPS. Ebselen potently protects lysosomal membrane integrity, preventing cathepsin-induced cleavage of SIRT 1 in EPCs and blunting SIPS and apoptotic cell death induced by relevant cardiovascular stressors. The proposed mechanism of SIRT1 depletion in stress has all of the attributes of being a paradigm of SIPS of EPCs. ***(Am J Pathol 2012, 180:973-983; DOI: 10.1016/j.ajpath.2011.11.033)***

Stress-induced premature senescence (SIPS) of endothelial cells has emerged as a notable contributor to global endothelial cell dysfunction (ECD) in diseases as diverse as diabetes, hypertension, chronic kidney disease, and atherosclerosis, to name a few.[1] We have previously demonstrated that critical cellular abnormalities preceding and mechanistically intimately linked to development of SIPS are characterized by lysosomal dysfunction manifesting in collapse of lysosomal pH gradient and lysosomal membrane permeabilization, and by subverted autophagy presenting as accumulation of giant autolysosomal vacuoles choking endothelial cells.[2,3]

Identification of the silent information regulator 2 (Sir2) in the yeast[4] and a subsequent demonstration of its role in delaying aging in *Saccharomyces cerevisiae*[5] have ignited interest in the role of members of this family in SIPS-related processes. Seven mammalian homologues of this NAD-dependent histone deacetylase have been identified with SIRT 1 and 2 expressed in the nucleus and the cytosol, SIRT 3–5 being mitochondrial proteins and SIRT 6 and 7 expressed in the nucleus.[6] It has been demonstrated that SIRT 1, abundant in embryonic stem cells, plays an essential role in regulating their self-renewal and resistance to stressors, like reactive oxygen species.[7–9] In addition, SIRT1 expression is one of the regulators of autophagy,[10] thus rais-

These studies were supported in part by NIH grants DK54602, DK052783, and DK45462, the Westchester Artificial Kidney Foundation (M.S.G.), and by Slovene Research Agency grants P1-0140 and J1-3602 (B.T.).

Accepted for publication November 22, 2011.

A guest editor acted as editor-in-chief for the manuscript. No person at Thomas Jefferson University was involved in the peer review process or final disposition of this article.

Address reprint requests to Michael S. Goligorsky, M.D., Ph.D., New York Medical College, Renal Research Institute, Basic Science Bldg., Room C-23, Valhalla, NY 10595. E-mail: Michael_goligorsky@nymc.edu.

ing a question of potential SIRT1 contribution to subverted autophagy in stressed endothelial and endothelial progenitor cells.

Endothelial progenitor cells (EPC) are not impervious to developing SIPS. Studies in db/db type 2 diabetic mice with the metabolic syndrome revealed premature senescence of bone marrow–derived EPC.[11] Chronic treatment with an antioxidant and peroxynitrite scavenger ebselen reversed SIPS *in vivo* and *in vitro*.[11–13] These data are in accord with the concept of "stem cell aging" as a basis for organismal aging.[14]

In the present study, we attempted to integrate the previous findings on endothelial SIPS with the exponentially growing field of SIRT1 effects on aging processes as applied to senescence of EPC. Specifically, we examined the impact of a range of relevant cardiovascular risk factors on the expression of SIRT1, along with development of SIPS and apoptosis, and documented the role of SIRT1 in the changes of cell viability. These findings were confirmed in mice with selective endothelial SIRT1 knockout. Furthermore, studies showed reciprocal relations between SIRT1 and p62 expression in stressed EPC, thus demonstrating an attendant abnormality of autophagy. The described effects of stressors could be partially mimicked by inducing lysosomal membrane permeabilization or by inhibiting autophagy and reversed by a cell-permeable inhibitor of cathepsins. Incubation of cathepsins B, S, and L with SIRT1 resulted in its proteolytic cleavage. We also inquired whether an antioxidant therapy combined with peroxynitrite scavenging (ebselen), shown in previous studies to protect endothelial cells and EPC from SIPS, exerts its effect via SIRT1 and, if it does so, what is/are the possible mechanism(s). The data presented here not only demonstrate the critical role of lysosomal membrane permeabilization followed by the release of cathepsins, cleavage, and depletion of SIRT-1 with the ensuing development of SIPS, but also establish ebselen as a potent protector of lysosomal membrane integrity that prevents cathepsin-induced cleavage of SIRT 1 in murine EPC, and we document its efficacy in preventing SIPS and apoptotic cell death induced by several relevant cardiovascular stressors.

Materials and Methods

Cell Culture

Murine EPCs were isolated from embryos at E7.5 to E7.8 of development and kindly provided by Dr. A Hatzopoulos[15]; these are referred to as eEPC to distinguish them from primary cultures of EPC. eEPC were repeatedly analyzed in the course of the study for an array of markers including FITC- or PE-conjugated anti-mouse CD117 (c-kit), CD150, Sca-1, CD34, CD31, CD44, CD45, Flk,−1, Tie2, Ulex Europaeus lectin, as well as antibodies to von Willebrand factor (vWF) and endothelial nitric oxide synthase (eNOS) followed by corresponding fluorescent secondary antibody (Jackson ImmunoResearch Laboratories, West Grove, PA) to ensure stability of their phenotype. EPC showed robust staining with Ulex Europaeus lectin and antibodies to vWF, but expressed low levels of Flk-1, CD31, CD34, and Sca-1, suggesting that the cells retained their nondifferentiated phenotype. All primary antibodies were produced by BD Biosciences (Rockville, MD) except for antibody to vWF (Dako North America, Carpinteria, CA) and to eNOS (Santa Cruz Biotechnology, Santa Cruz, CA). Data were acquired using a FACScan cytometer equipped with a 488-nm argon laser and a 620-nm red diode laser and analyzed using CellQuest software (Becton Dickinson, San Jose, CA). The setup of FACScan was performed using unstained and single antibody–stained cells. EPC were plated on 0.1% gelatin-coated plates and maintained at 37°C and 5% CO_2 in DMEM culture medium containing 20% heat-inactivated serum (55°C 30 minutes; Invitrogen, Carlsbad, CA), 0.1 mmol/L 2-mercaptoethanol, 1 mmol/L MEM nonessential amino acids (Invitrogen, Grand Island, NY), 100 U/mL penicillin and 100 μg/mL streptomycin, 2 mmol/L L-glutamine (Invitrogen), and 2 mmol/L HEPES, pH 7.5.

Mice with Endothelial SIRT1 Deletion

An endothelial SIRT1-deleted mouse model ($Sirt^{endo-/-}$ or $Sirt^{endo+/-}$) was developed by cross-breeding of CBy.129(B6)-*Sirt1*^{tm1Ygu}/J (homozygous for targeted allele SirT1co/co, viable and fertile, containing a loxP-flanked neomycin cassette upstream and downstream of exon 4 of the targeted gene) with the Tie2-Cre transgenic mice (both from Jackson Laboratories, Bar Harbor, ME).[16] These mice thrive similar to their wild type and heterozygote littermates (Mendelian distribution of offspring), have normal blood pressure at age of 8 weeks, but exhibit a mild impairment in vasorelaxation and moderate impairment in *ex vivo* angiogenesis (manuscript in preparation).

Bone marrow–derived mononuclear cells (MNCs) were obtained according to previously described procedure using Histopaque 1077 (ICN, Costa Mesa, CA) gradient centrifugation.[11] Isolated bone marrow MNCs were washed three times with EGM-2 medium (Cambrex, Walkersville, MD) supplemented with 2% penicillin/streptomycin (Invitrogen), and 0.25 μg/mL amphotericin B (Invitrogen). MNCs were resuspended in 3 mL complete EGM-2 medium and seeded onto a 35-mm tissue culture dishes precoated with pronectin (Sigma-Aldrich, St. Louis, MO) at 37°C, 5% CO_2, in a humidified incubator. After 24 hours in culture, nonadherent cells and debris were aspirated, adherent cells were washed once with complete EGM-2 medium, and complete EGM-2 medium was added to each well. Medium was changed daily for 7 days and then every other day until the first passage. EPC were assayed by co-staining with acetylated LDL (acLDL)-DiI (Biomedical Technologies, Stoughton, MA) for 3 hours at 37°C and FITC-conjugated *Ulex europaeus* lectin (Sigma-Aldrich) for 30 minutes at 37°C, both of which are features characteristic of endothelial lineage.

Detection of Senescent and Apoptotic Cells

Senescence-associated β-galactosidase (SA β-gal)–positive cells were detected by cytochemical staining

at pH 6.[17] Stained cells were viewed under an inverted microscope at ×200 magnification. The number of SA-β-gal–positive cells per total number of cells in the same field was determined by counting at least eight random fields for each sample under bright-field illumination. Detection of SA β-gal in the *en face* aortic preparations was performed using a previously described protocol.[18]

A Caspase Detection Kit (Calbiochem, La Jolla, CA) was used to detect activated caspases in cultured cells. The FITC-labeled caspase inhibitor benzyloxycarbonyl Val-Ala-aspartic acid fluoromethyl ketone (VAD-FMK) irreversibly binds to activated caspases 1 to 9. In brief, cells were incubated in FITC-VAD-FMK containing culture medium (1:300, vol:vol) for 0.5 to 1 hour in 37°C incubator with 5% CO_2. To detect apoptosis by fluorescence microscopy, cells were co-stained with Hoechst 33342 (Sigma, St. Louis, MO). The data presented were obtained by counting the proportion of apoptotic cells per 2000 cells using fluorescence microscopy (in each experiment, at least 15 to 20 randomly chosen fields were examined). To detect apoptosis by flow cytometry, cells were re-suspended in PBS containing 1 μg/mL propidium iodide (PI, Molecular Probes, Eugene, OR). FAM-VAD-FMK and PI fluorescence was measured by FACScan (Becton Dickinson, San Jose, CA).

Western Blot Analysis

Cells were treated with H_2O_2, asymmetric dimethylarginine (ADMA) and nonenzymatically glycated long-lived protein, collagen I (GC), or their respective controls, symmetric dimethylarginine and native collagen I (SDMA and NC, respectively) 3 days after the last change of the culture medium. Cell lysates were prepared in a buffer containing 50 mmol/L Tris, pH 7.4, 100 mmol/L NaCl, 0.1% SDS, 0.5% sodium deoxycholate, 1% NP-40, and protease inhibitor cocktail (Roche, Indianapolis, IN). Lysates were assayed for total protein concentration (BCA assay, Pierce, Rockford, IL). SDS-PAGE was performed using 4% to 20% Tris-glycine gels (Invitrogen) under reducing conditions with 10 to 30 μg of total protein used from each sample for electrophoresis followed by electrotransfer to Immobilon-P (Millipore, Billerica, MA) membrane. Secondary HRP-conjugated antibody was used at a dilution of 1:2000. The membranes were incubated with primary antibodies overnight in a cold room, followed by HRP-conjugated IgG, and were visualized with an enhanced chemiluminescence detection system (Pierce). Primary anti-mouse SIRT1 polyclonal antibody (Millipore, Billerica, MA), anti-mouse Atg5 monoclonal antibody (R&D Systems, Minneapolis, MN), anti–acetyl lysine polyclonal antibody (Abcam, Cambridge, MA), and anti–β-tubulin monoclonal antibody (Sigma) was used at the dilution of 1:1000. Primary anti-p62/SQSTM-1 antibody (Abnova, Walnut, CA) was used at 1:10,000, whereas primary anti-GST antibody (GE Healthcare, Piscataway, NJ) at 1:5000. Secondary HRP-conjugated antibodies were used at a dilution of 1:2000. Protein A/G PLUS-Agarose beads for immunoprecipitation was ordered from Santa Cruz Biotechnology (Santa Cruz, CA).

SIRT1 Expression Plasmid and Short Hairpin RNA

The plasmid pUSeAmp-Sir2α was obtained from Millipore. Four short hairpin RNA (shRNA) constructs against Mus musculus SIRT1 (#TR505485), and the 29-mer scrambled shRNA cassette in pRS Vector were purchased from Origene Technologies (Rockville, MD) and used according to the manufacturer's recommendations. To ensure efficiency and specificity, all constructs were tested by transfecting EPC and the endogenous SIRT1 level monitored by Western blot analysis. Cells were suspended in mouse ES Cell Nucleofector Solution (VPH-1001; Lonza, Cologen, Germany) to a final concentration of 1 to 5×10^6 cells/100 μl. The cells were transfected using 2 to 10 μg of shRNA by electroporation in Amaxa certified cuvettes, program A-023. The cells were transferred to the prewarmed medium and incubated for indicated periods of time at 37°C with 5% CO_2.

Lysosomal pH and Intracellular Cathepsin Detection

Lysosomal pH was monitored using a metachromatic fluorophore acridine orange, as previously reported.[3] The activity of intracellular cathepsin B in eEPC was monitored using Magic Red (MR) Cathepsin detection kit using the fluorophore cresyl violet (Immunochemistry Technologies, Bloomington, IN). EPC were loaded with this cathepsin substrate for 1 hour at 37°C in 5% CO_2 in the culture medium containing MR-Cathepsin solution at 1:260 dilution.[19] After loading, cells were washed twice with PBS, and intracellular localization of the hydrolyzed (fluorescent) MR product was examined using fluorescence microscopy (Nikon Eclipse E800) at an excitation 540 nm and emission 590 nm at ×600 magnification. The subcellular MR fluorescence intensity was analyzed using line-scan function routines of MetaVue software. The average signal intensity in cytosolic and lysosomal compartments was normalized against the background and their ratio was calculated. At least 20 images were analyzed for each treatment and each experiment was repeated at least three times.

SIRT1 Cleavage by Cysteine Cathepsins

Recombinant human cysteine cathepsins B, L, and S were prepared as described previously,[20–22] and active site titrated,[23] whereas recombinant SIRT1 was prepared as a fusion protein with GST as described above. Cleavage of SIRT1 (1.47 μmol/L final concentration) by cathepsins B, L, and S (0.57 μmol/L final concentration) was analyzed essentially as described previously.[24] As a positive control GST (3.8 μmol/L) was included.

Statistical Analysis

All experiments were repeated at least three times. Values are given as mean ± SE. Data were analyzed using analysis of variance with *post hoc* analysis for multiple group comparisons using Bonferroni method. A P value of <0.05 was considered statistically significant.

Results

Effects of Cardiovascular Stressors on EPC Viability and SIRT1 Expression

Previous studies have demonstrated that cardiovascular risk factors used herein promoted SIPS and/or apoptosis in mature endothelial cells[12] eventuating in vasculopathy. Therefore, we inquired whether similar phenomena are observed in endothelial progenitor cells. A range of relevant cardiovascular stressors encompassing an inhibitor and uncoupler of eNOS, asymmetric dimethylarginine (ADMA, 5 μg/mL), an advanced glycation endproduct (AGE)–modified long-lived protein, collagen I (GC, 100 μmol/L), and a pro-oxidant hydrogen peroxide (H_2O_2, 50 to 100 μmol/L) were applied to embryonic EPC for 24 to 72 hours. As summarized in Figure 1, all stressors significantly increased the proportion of apoptotic and prematurely senescent EPC.

The existing evidence linking senescence to the expression of sirtuins and, in particular, SIRT1, prompted us to examine the expression of this protein deacetylase in embryonic EPC. Application of each of three stressors was associated with a significant decline in the expression of SIRT1 (Figure 2). The similar decline in SIRT1 expression was observed in human umbilical vein endothelial cells and in mouse hemangioendothelioma endothelial cells (not shown).

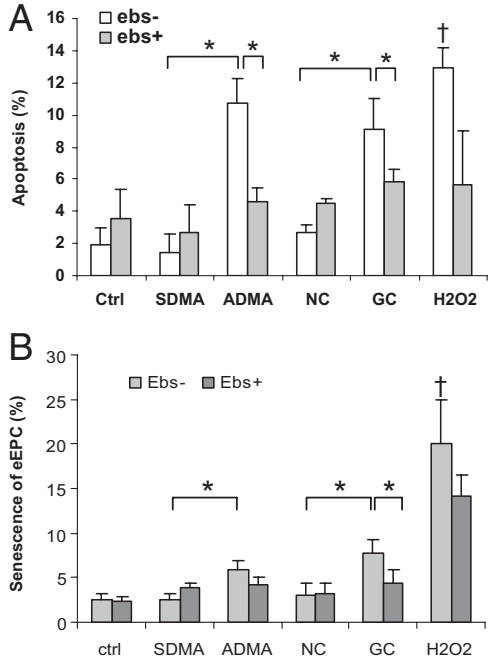

Figure 1. Treatment with GC, ADMA, or H_2O_2 induces apoptosis and senescence in eEPC. After 3 days of treatment with GC, ADMA, or H_2O_2, significant increases in proportion of apoptotic (**A**) and senescent (**B**) cells occurred compared with their individual control groups: native collagen (NC), symmetric dimethylarginine (SDMA), and control untreated cells (Ctrl). Co-application of ebselen (ebs) with GC, ADMA, or H_2O_2 (ebs+) prevents apoptosis. Ebselen also prevents premature senescence induced by GC (**B**). Data are mean ± SD of five independent experiments. $^*P < 0.05$; $^\dagger P < 0.05$ compared with Ctrl/ebs−.

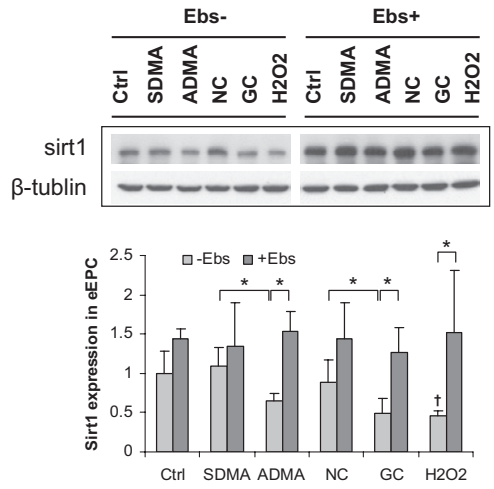

Figure 2. SIRT1 expression in eEPC after co-application of GC, ADMA, or H_2O_2 with ebselen (ebs). Western blot analysis demonstrated reduced SIRT1 level in EPC after 3 days of treatment with GC, ADMA, or H_2O_2. Co-treatment with ebselen prevented the observed effect. The results of densitometric analysis are shown in relative units compared with Ctrl/ebs−. Data are means ± SD of six independent experiments. $^*P < 0.05$; $^\dagger P < 0.05$ compared with Ctrl/ebs−.

These data raise a question of causality between changes in SIRT1 expression and EPC viability: Namely, is SIRT1 depletion sufficient and necessary to account for increased SIPS and apoptosis and could its overexpression prevent these outcomes of cell stress? To address this question, we manipulated SIRT1 expression genetically or pharmacologically, alone or in combination with the stressors, and monitored cell viability. Overexpression of SIRT1 did not affect basal rate of apoptosis or SIPS in embryonic EPC; however, the proportion of apoptotic cells was significantly reduced in SIRT1-transfected cells subjected to each of the stressors, whereas the proportion of SIPS in embryonic EPC was significantly decreased in ADMA-treated cells (Figure 3, A and B). In contrast, repression of SIRT1 with shRNA construct resulted in a significant increase in SIPS cells under basal conditions, enhanced apoptosis even under control conditions (Ctrl, SDMA, and NC groups), and further enhanced apoptosis in GC group (Figure 3C). An increase in SIPS was seen in Ctrl and NC groups following shRNA/SIRT1 transfection (Figure 3D). Results obtained with an inhibitor of SIRT1, sirtinol are summarized in Figure 3F. Sirtinol, 100 μmol/L, resulted in increased proportion of senescent eEPC under all basal conditions. Thus, both the SIRT1-targeted "gain-of-function" and "loss-of-function" experiments supported its role in protection and destruction, respectively, of embryonic EPC cultured in the presence and even absence of noxious stimuli.

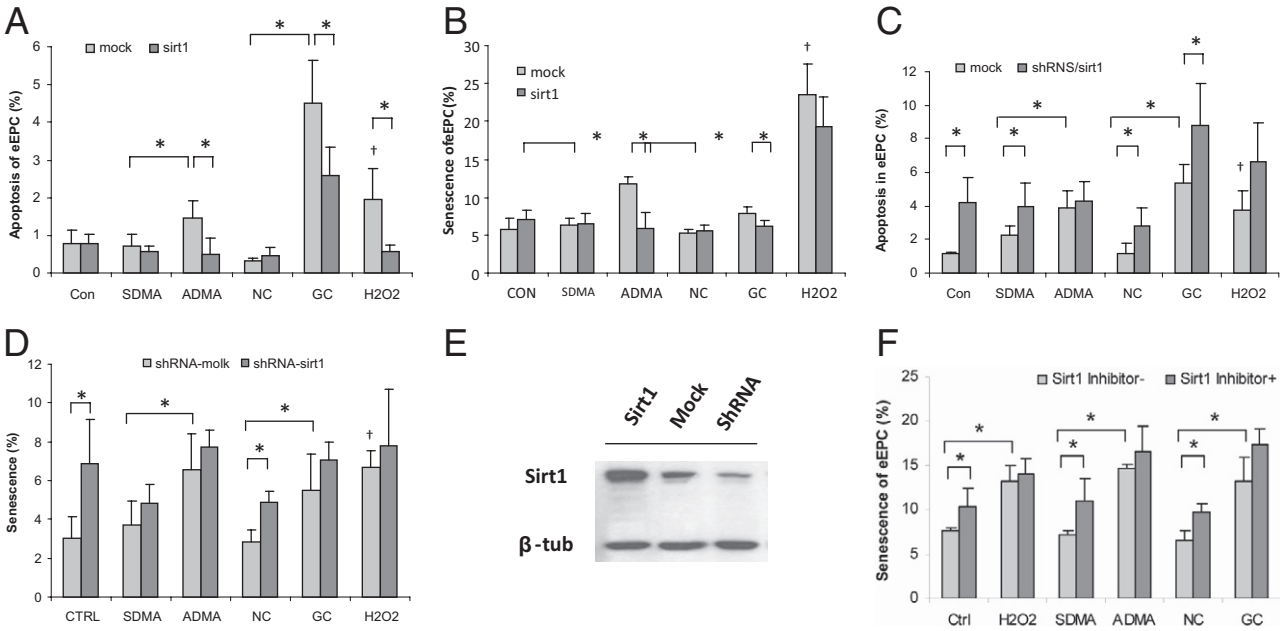

Figure 3. Apoptosis and senescence of eEPC after transfection of SIRT1 plasmid or shRNA/SIRT1 construct. **A** and **B:** Overexpression of SIRT1 prevented apoptosis induced by ADMA, GC, or H_2O_2 (**A**) and SIPS induced by ADMA or GC (**B**). **C** and **D:** In contrast, decreasing SIRT1 level with shRNA (shRNA/SIRT1) enhanced apoptosis even under control conditions as show in Ctrl, SDMA, and NC groups, and further enhanced apoptosis in GC group (**C**). An increase in SIPS was seen in Ctrl and NC groups after shRNA/SIRT1 transfection (**D**). **E:** Representative Western blot analysis of SIRT1 expression after its overexpression (SIRT1), inhibition (shRNA), and control transfection, mock-control (Mock). **F:** Alternatively, cells were treated with the inhibitor Sirtinol at 100 μmol/L, which resulted in increased proportion of senescent eEPC under basal conditions. Data are mean ± SD of five independent experiments. $^*P < 0.05$; $^\dagger P < 0.05$ compared with Ctrl/ebs−.

Senescence of Endothelial and Endothelial Progenitor Cells Obtained from Mice with Endothelial SIRT1 Knockout

To test the validity of above cell culture findings in a whole-animal system, we generated mice with endothelial deletion of SIRT1. Mice with Tie-2–driven endothelial and EPC SIRT1 deletion were used at age 3 to 4 months to obtain EPC and examine progenitor and mature endothelial cells for the possible premature senescence. Bone marrow–derived EPC, after a 3-week-long *in vitro* expansion, exhibited *in vitro* an almost twofold increase in the frequency of prematurely senescent cells under basal conditions in heterozygote and homozygote mice ($Sirt^{endo+/-}$ and $Sirt^{endo-/-}$), whereas the frequency of activated caspase-positive cells was elevated only in homozygote SIRT1-deletion mice ($Sirt^{endo-/-}$) (Figure 4A). Whole-mount *en face* thoracic aortic preparations, obtained from mice at age 3 to 4 months, were stained for SA-β-gal expression. Endothelial SIRT1-deleted aortas exhibited a robust staining for SA-β-gal in endothelial cells located in the plane of aorta and at the orifices of intercostal arteries, whereas neither wild-type nor heterozygote littermates showed SA-β-gal positivity at these locations (Figure 4, B and C). These findings confirm *in vitro* observations made in the established progenitor cell line on the role of SIRT1 depletion in the acquisition of senescent phenotype.

Ebselen Prevents Down-Regulation of SIRT1 by Cardiovascular Stressors

Pursuant to the previous finding that a selenoorganic peroxynitrite scavenger, ebselen, improves viability of stressed HUVEC and embryonic EPC,[11] we next examined the possibility that the observed effect is related to modulation of SIRT1. Indeed, EPC subjected to ADMA, GC, or H_2O_2 in the presence of ebselen showed a significant attenuation of apoptosis, whereas SIPS was significantly reduced in embryonic EPC subjected to GC or H_2O_2 (Figure 1). Co-application of ebselen with ADMA, GC, or H_2O_2 was associated with normalization of SIRT1 expression, otherwise profoundly suppressed by these stressors (Figure 2).

Effects of Cardiovascular Stressors Are Mediated via Induction of Lysosomal Membrane Permeabilization

One of the targets of deacetylase activity of SIRT1 is represented by members of autophagic proteins Atg 5 and 7.[10] Therefore, it could be expected that one of the consequences of SIRT1 depletion in stressed EPC is manifested as impaired autophagy. Indeed, subverted autophagy was found in our previous work in stressed HUVEC.[5] Because the abundance of Sequestosome-1 protein, p62/SQSTM-1, which targets proteins destined for degradation to form aggregates and sequester in autophagosomes to be later degraded in autolysosomes,[25] reflects the intensity of autophagic flux, we next

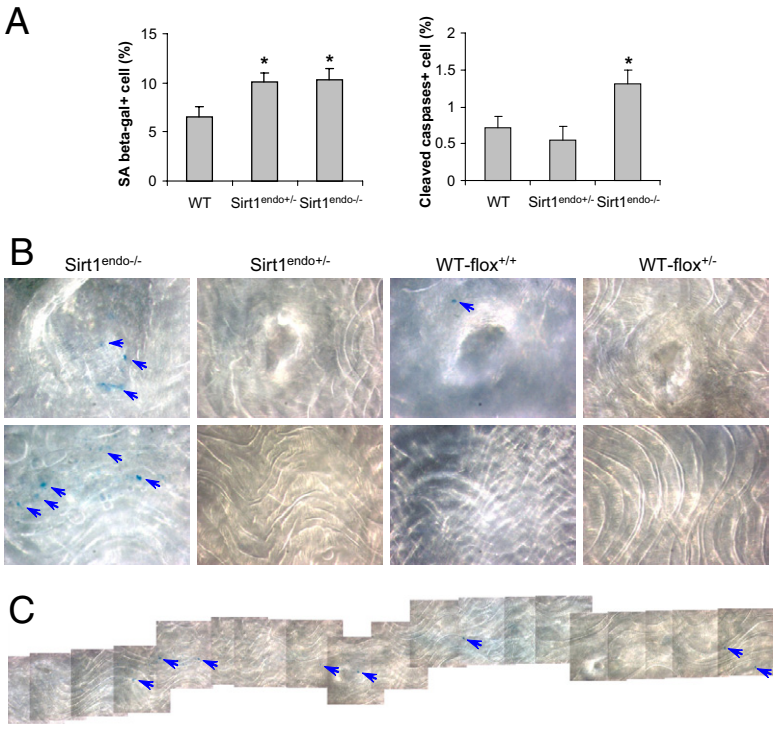

Figure 4. Cleaved caspases and SA-β-galactosidase staining of bone marrow–derived EPC and SA-β-galactosidase staining of aortic endothelial cells in endothelial SIRT1-deleted and control mice. **A:** Proportion of SA-β-galactosidase–positive and activated caspase–positive EPC isolated from the bone marrow of $Sirt^{endo-/-}$, $Sirt^{endo+/-}$, and wild-type mice ($WT\text{-}flox^{+/+}$ and $WT\text{-}flox^{+/-}$). **B:** *En face* aortic staining for SA-β-galactosidase reveals minimal staining in control and heterozygotic mice and massive clusters of stained cells in endothelial SIRT1 knockout mice. Representative images of orifices to intercostals arteries and the plain portion of the thoracic aorta of controls and endothelial SIRT1-deleted mice. Original magnification, ×60. **C:** Representative composite of consecutive images reconstructing the length of *en face* thoracic aorta obtained from a 4-month-old endothelial SIRT1 knockout mouse, depicting frequency of clusters of SA-β-gal–positive cells. Original magnification, ×60. **Arrows** indicate cells stained for SA-beta-galactosidase.

examined the possibility of its accumulation in stressed embryonic EPC. The endogenous p62/SQSTM-1 expression level was elevated in eEPC after 24 hours of ADMA and H_2O_2 treatment (Figure 5A), and after 72 hours of GC treatment (Figure 5A). Co-application of ebselen prevented changes in p62/SQSTM-1 in all treatment groups and at all time points, thus suggesting that stress to embryonic EPC is associated with the impaired autophagy and this impairment is mitigated by ebselen. Indeed, testing the ability of stress-induced SIRT1 depletion to lead toward impaired Atg5 deacetylation, we next examined the abundance of acetylated Atg5. As shown in Figure 5B, immunoblotting of immunoprecipitated Atg5 with the antibodies against acetylated lysine demonstrated that one of the stressors used, GC, shown to deplete SIRT1, led to the increase in the level of acetylated Atg5, whereas co-application of ebselen prevented it.

Lysosomal membrane permeabilization and dysfunction induced by diverse stressors has been identified as

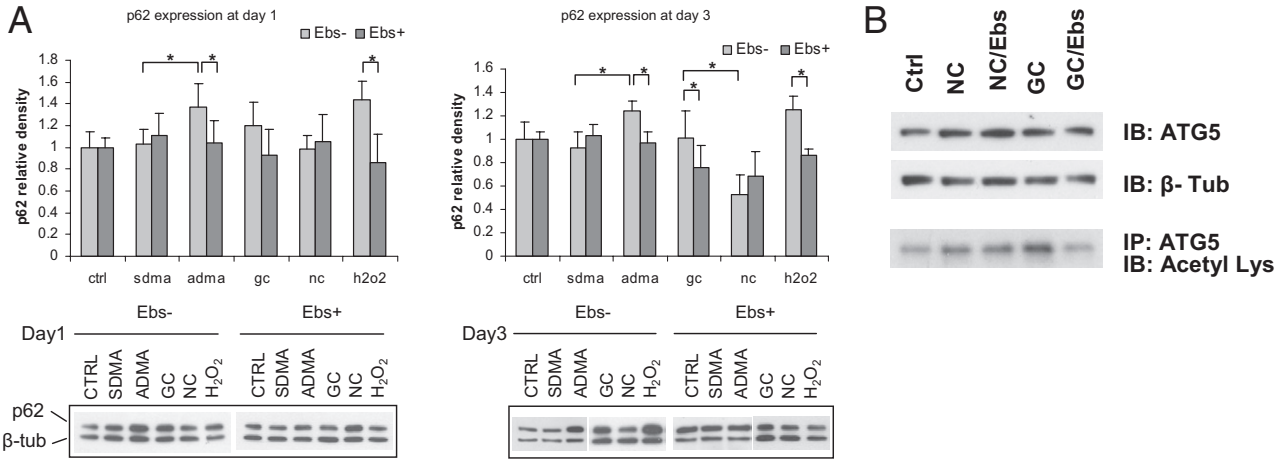

Figure 5. Dysfunctional autophagy of eEPC after GC, ADMA, or H_2O_2 treatment. **A:** Levels of p62. Endogenous p62 expression level was elevated in eEPC after 24 hours ADMA and H_2O_2 treatment (**A**, **left panel**) and after 72 hours of GC treatment (**A**, **right panel**). Co-application of ebselen (ebs) prevented changes in p62 in all treatment groups and at all time points. Results of densitometry analysis are shown in relative units compared with Ctrl/ebs−. Data are mean ± SD of four independent experiments. $^{*}P < 0.05$; $^{\dagger}P < 0.05$ compared with Ctrl/ebs−. **B:** Analysis of acetylated Atg5 in eEPC by immunoprecipitation and immunoblotting. Atg5-Atg12 protein complex (56 KDa) was precipitated from eEPC cell lysates using monoclonal anti-mouse Atg5 antibody and protein A/G PLUS-Agarose beads. Acetylation was analyzed by immunoblotting using polyclonal anti–acetyl lysine antibody. The amounts of cell lysate used for immunoprecipitation in each group were balanced first by protein concentration followed for confirmation by immunoblotting using β-tubulin (55 KDa) and Atg5-Atg12 antibodies. Data are representative of two separate experiments.

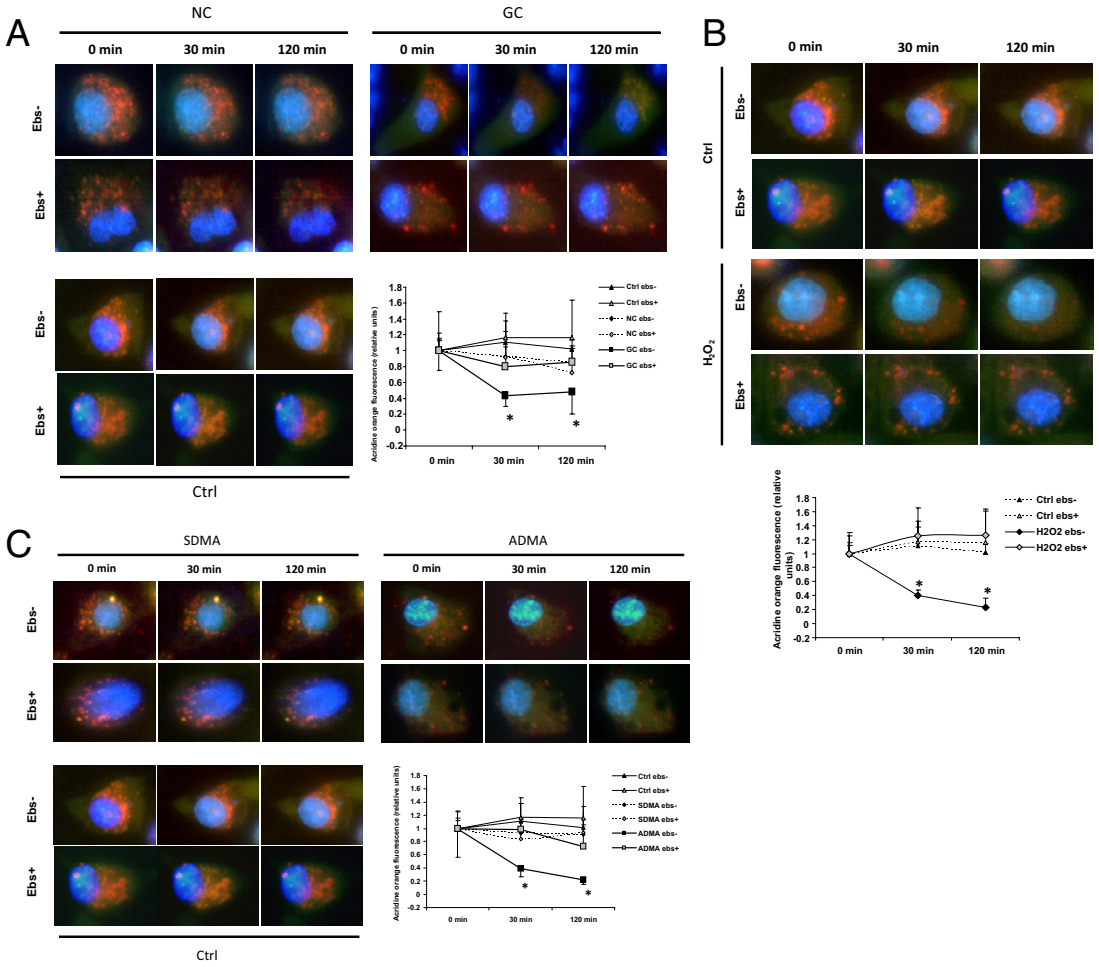

Figure 6. Lysosomal membrane permeabilization in EPC exposed to stressors. **A:** GC triggers lysosomal pH collapse. After incubation in 1 μmol/L acridine orange for 15 minutes, the fluoroprobe was detected as a red-punctuated fluorescence signal in intact cells, as shown in control. When the cells were exposed to GC, the punctuated fluorescence pattern nearly disappeared in the span of 2 hours, whereas it was preserved in cells treated with NC. Treatment with ebselen prevented changes induced by GC. **Lower right panel** shows quantification (ratio) of red acridine orange fluorescence signal intensity in lysosomes against cytosolic green fluorescence. The relative fluorescence intensity was adjusted to the intensity at 0 minute for each individual treatment group. Data are mean ± SD of three independent experiments. $^*P < 0.05$ compared with GC/ebs− and NC groups. **B:** H_2O_2 triggers lysosomal pH collapse. Experimental conditions as in **A**. Relative fluorescence intensity was adjusted to the intensity at 0 minutes for each individual treatment group. Data are mean ± SD of three independent experiments. $^*P < 0.05$ compared with H_2O_2/ebs−. **C:** ADMA triggers lysosomal pH collapse. Experimental conditions as in **A**. $^*P < 0.05$ compared with ADMA/ebs− and SDMA groups.

one of the causes for subversion of autophagy[26] and Patschan et al[2,3] observed subverted autophagy in HUVEC exposed to GC. To assess the possibility that impaired autophagy in embryonic EPC could be related to stressor-induced lysosomal membrane permeabilization, we next performed time-lapse microscopy of acridine orange-labeled embryonic EPC, as previously detailed.[3] Using this metachromatic fluorophore that emits red/orange at low pH values and green at a neutral pH, we demonstrated that all three stressors induced collapse of lysosomal pH gradient and lysosomal membrane permeabilization (Figure 6, A–C) manifesting in the reduction of punctated orange fluorescence pattern and acquisition of diffuse green cytosolic fluorescence. Coapplication of ebselen with the stressors resulted in a remarkable preservation of lysosomal membrane integrity, consistent with the prevention of oxidant-induced lysosomal membrane permeabilization.

Lysosomal Membrane Permeabilization Results in SIRT1 Depletion

Therefore, the question we asked next was: Does a primary abnormality in lysosomal membrane permeability or a subversion of autophagy affect the level of SIRT1? Lysosomal pH gradient collapse and membrane permeability was induced by treating embryonic EPC with a lysosomotropic alkaline proton pump inhibitor, chloroquine (30 μmol/L). This treatment did not result in the accumulation of p62/SQSTM-1 within 24 hours and at this time SIRT1 expression was unchanged from control (Figure 7). However, by 72 hours, chloroquine resulted in accumulation of p62/SQSTM-1 and significant reduction of SIRT1. In parallel experiments, 3 methyladenine (4 mmol/L), an inhibitor of class III phosphatidylinositol-3-kinase necessary for induction of autophagy,[27] was used as an inhibitor of autophagy. This

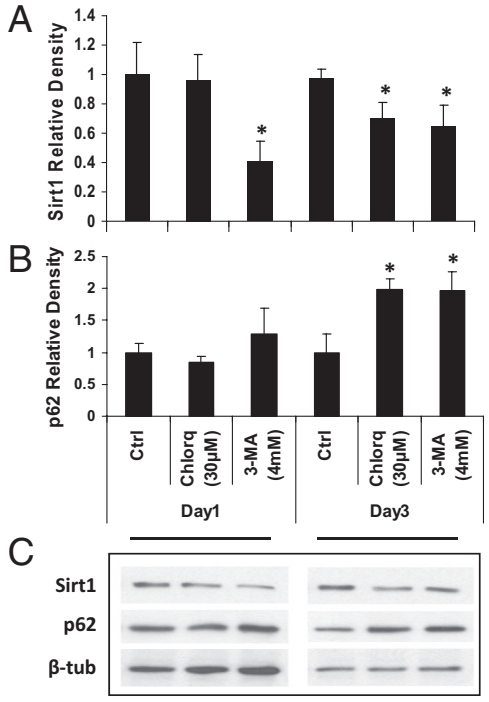

Figure 7. Changes of lysosomal permeability influence the endogenous level of SIRT1 and p62. Treatment of eEPC for 24 to 72 hours with chloroquine (chlor, 30 μmol/L) or 3-MA (4 mmol/L), suppressed SIRT1 expression level (**A** and **C**). In contrast, p62 showed significant accumulation after 72 hours of treatment with chloroquine or 3-MA (**B** and **C**). Results of densitometry analysis (**A** and **B**) are shown in relative units compared with control at day 1 or day 3. Data are mean ± SD of four independent experiments. $^*P < 0.05$ compared with their corresponding controls on day 1 or 3.

treatment resulted in the suppression of SIRT1 levels on days 1 and 3, whereas significant accumulation of p62/SQSTM-1 was detectable at day 3. Hence, these studies are supportive of the idea that lysosomal dysfunction is at least in part responsible for SIRT1 depletion eventuating in subverted autophagy in stressed embryonic EPC.

Role of Cathepsins in SIRT1 Degradation

The above findings are suggestive of the leaked lysosomal contents, including cathepsins, that could affect SIRT1 levels, either directly or indirectly. To test this possibility, embryonic EPC were subjected to the above cardiovascular stressors in the presence of E64d, a broad-spectrum cell-permeable inhibitor of cysteine cathepsins.[28] As shown in Figure 8A, this treatment resulted in a significant blunting of SIRT-1 depletion associated with exposure to ADMA, GC, and H_2O_2. Moreover, E64d pretreatment of embryonic EPC significantly reduced SIPS and apoptosis induced by oxidative stress (Figure 8B). These findings, in conjunction with the demonstration of stress-induced lysosomal dysfunction and subversion of autophagy, argue in favor of the involvement of lysosomal membrane permeabilization[26] in triggering SIPS or apoptotic cell death.

To test further the idea of lysosomal membrane permeabilization, we used a cathepsin B substrate that acquires fluorescence on cleavage, Magic Red,[19] to visualize cathepsin B translocation to the cytoplasm (Figure 9). Image analysis data demonstrated elevated level of cytoplasmic fluorescence intensity, with the ratio of cytoplasmic:lysosomal fluorescence intensities consistently increased after induction of cell stress, but blunted by co-application of ebselen. These finding further confirm lysosomal membrane permeabilization on stress and demonstrate the release of cathepsin B from the lysosomal compartment to the cytosol. In addition, the data support the argument that the observed SIRT1 preservation by ebselen may be due to its prevention of stress-induced lysosomal membrane permeabilization.

To directly verify the possibility of cathepsin cleavage of SIRT1, degradation of recombinant SIRT1 by cysteine cathepsins B, L, and S was investigated *in vitro* at neutral pH. The major reason to select these three cathepsins was that cathepsins B and L are the most abundant and ubiquitously expressed cysteine cathepsins, whereas cathepsin S is also found in endothelial cells, in addition to

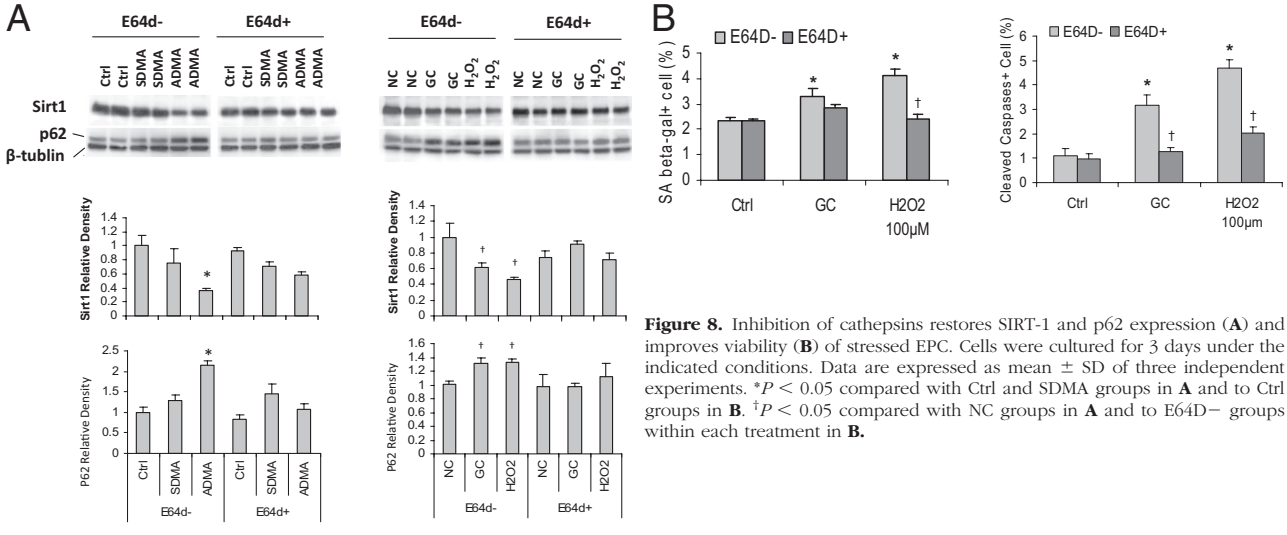

Figure 8. Inhibition of cathepsins restores SIRT-1 and p62 expression (**A**) and improves viability (**B**) of stressed EPC. Cells were cultured for 3 days under the indicated conditions. Data are expressed as mean ± SD of three independent experiments. $^*P < 0.05$ compared with Ctrl and SDMA groups in **A** and to Ctrl groups in **B**. $^\dagger P < 0.05$ compared with NC groups in **A** and to E64D− groups within each treatment in **B.**

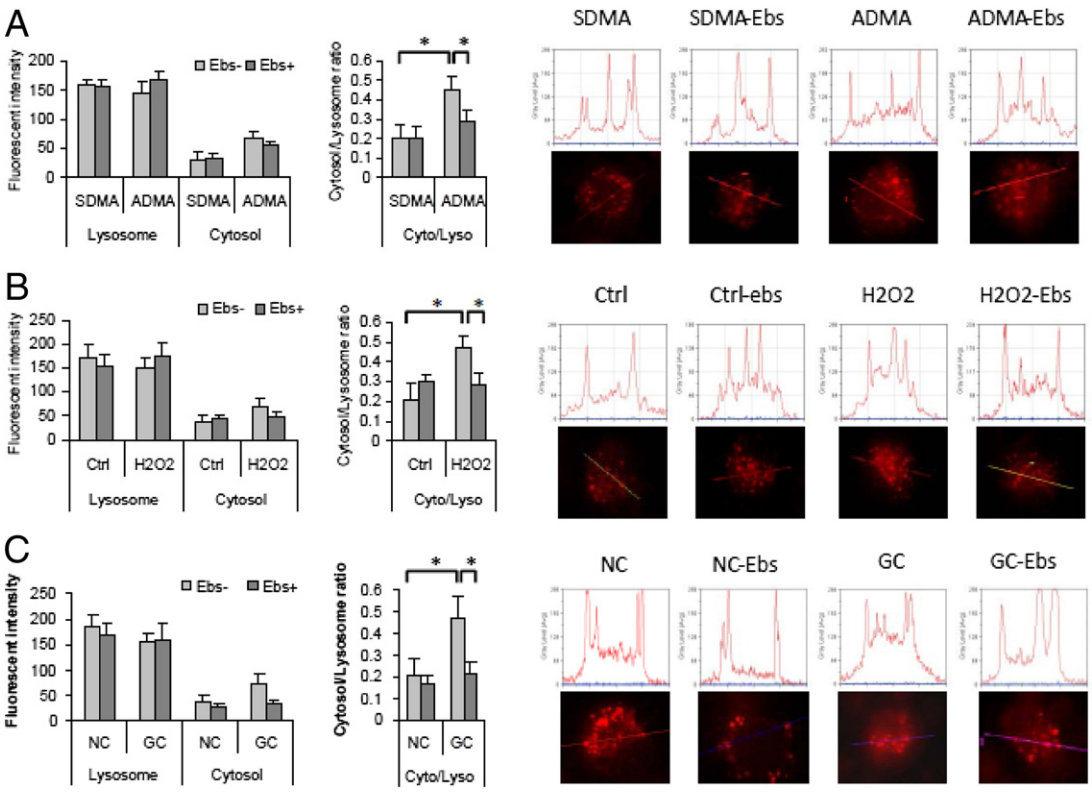

Figure 9. Leakage of cathepsin B from the lysosomal compartment to the cytosol and preventive effect of co-application of ebselen with the stressors; **A:** ADMA; **B:** hydrogen peroxide; **C:** glycated collagen). **Upper panels** in **A** and **B**, and **left panel** in **C**, summarize relative fluorescence intensities. Corresponding **lower** and **right panels** of **A**, **B**, and **C** illustrate representative cells (of 20 to 50 each) and line scanning of fluorescence intensity over lysosomes and cytosol. Data are mean ± SD of three independent experiments. $^*P < 0.05$.

being the most stable at neutral pH among all of the cathepsins. As shown in Figure 10, all three cathepsins cleaved and degraded SIRT1, supporting the hypothesis that cysteine cathepsins are directly responsible for SIRT1 degradation in EPC. Notably, the size of SIRT1 fragments differed with the use of different cathepsins, in accord with their specific cleavage profiles. The cleavage within SIRT1 protein and not within the GST moiety was additionally confirmed by Western blotting against GST, which helped to distinguish the fragmentation pattern of SIRT1 from that of GST.

Discussion

Data presented herein demonstrated that SIRT1 depletion occurring in stressed embryonic EPC is causatively linked to induction of SIPS and apoptosis of these cells. These findings buttress the concept of "stem cell aging" as a prerequisite for organismal aging.[14] Because the goal of the present study was to define protracted consequences of cell stress rather than its acute effects, which are known to induce SIRT1 system, the timing of the studies performed here was postponed 1 to 3 days after the application of stressors. Reciprocal relations between SIRT1 expression and the level of p62/SQSTM-1, a marker of autophagic flux, in combination with lysosomal membrane permeabilization implied that autophagy is subverted in stressed embryonic EPC, similar to what previously has been observed in cultured endothelial cells.[3] The key role of SIRT1 deficiency in premature senescence of endothelial and endothelial progenitor cells was confirmed *in vivo* and *in vitro* in mice

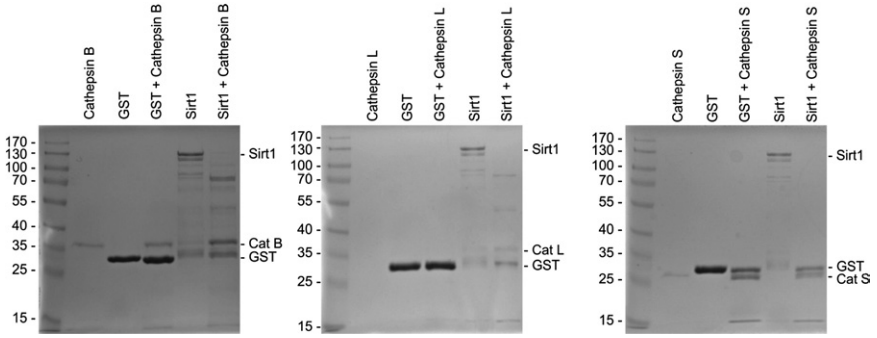

Figure 10. *In vitro* cleavages of recombinant SIRT1 by cathepsins at pH 7.2 and 37°C. Experimental details are given in *Materials and Methods*. Recombinant GST, SIRT1-GST, and cathepsins B, L, and S were used as negative controls and are marked with lines. Cathepsin-treated GST was used as a positive control. Partial degradation of Sirt1 was observed with cathepsin B, whereas cathepsin S was found to completely degrade Sirt1-GST, leaving only partially processed GST. Cathepsin L was slightly less efficient than cathepsin S.

with endothelial SIRT1 deletion: EPC obtained from these animals showed increased frequency of SA-β-gal–positive and activated caspase-positive cells under basal conditions; and aortic endothelium in whole-mount *en face* preparations showed increased SA-β-gal positivity. One of the proximal causes for subverted autophagy was identified as lysosomal membrane permeabilization. In fact, a direct permeabilization of lysosomes *per se* mimics the stress-induced reciprocal relations between SIRT1 and p62/SQSTM-1. Moreover, blockade of cathepsins activity with E64d prevented stress-induced depletion of SIRT1 and SIPS (induced by hydrogen peroxide or GC), further supporting the role of lysosomal membrane permeabilization in SIRT1 depletion. Elevated cytoplasmic activity of cathepsin B, as judged from the imaging data obtained with the fluorescent substrate, Magic Red, further supported the possibility of the involvement of cathepsin in SIRT1 depletion. This mode of action was directly confirmed in the *in vitro* co-incubation of SIRT1 with cathepsins B, L, and S. Furthermore, considering the role of oxidative stress in lysosomal membrane permeabilization, we applied a selenoorganic antioxidant and peroxynitrite scavenger, ebselen, which protected SIRT1 from stress-induced depletion by preventing the loss of lysosomal membrane integrity and, therefore, reducing cytoplasmic shift of cathepsins. Collectively, the data outline a pathway from stressed embryonic EPC via oxidative stress to lysosomal membrane permeabilization, followed by SIRT1 depletion secondary to leaked cathepsins (Figure 11). This pathway may be linked to subverted autophagy, which serves as an amplifier for SIPS. Ebselen, by preventing oxidative stress-induced loss of lysosomal membrane integrity, blocks this pathway. Although each step of the pathway may have multiple mechanistic branching, the outline rendered here appears to provide the best fit of the data.

It has been established that lysosomal dysfunction is a frequent accompaniment of cell stress.[29,30] Moreover, lysosomal destabilization is caused by reactive oxygen species,[31,32] known to be induced by all three stressors used in the present studies.[3,12,33] In this context, effects of ebselen, a selenoorganic antioxidant and peroxynitrite scavenger, are conceivably mediated through reduction of free radical–induced lysosomal membrane permeabilization, and data presented herein confirm this prediction.

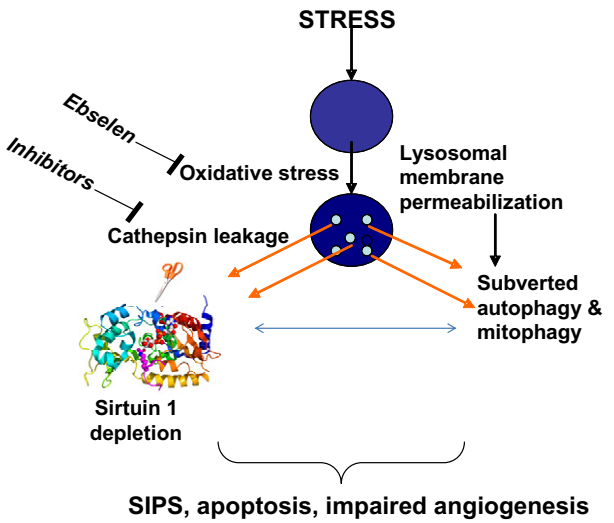

Figure 11. Hypothetical pathway of SIPS induction in EPC by relevant cardiovascular stressors.

Lysosomal dysfunction is known to subvert autophagy leading to accumulation of autophagosomes/autolysosomes, as well as the engulfed material (lipofuscin-loaded lysosomes), because of the lack of the final recycling step.[34] When this loss of function is accompanied by the lysosomal membrane permeabilization, the cathepsins released into the cytosol may trigger apoptosis and redirect the normally compartmentalized autophagy to nonphysiological sets of targets. The molecular mechanisms by which cathepsins trigger apoptosis are not entirely clear; however, there is accumulating evidence that they activate Bid and degrade antiapoptotic members of the Bcl-2 family, resulting in the engagement of mitochondrial pathways in cell death.[24] Here we demonstrate for the first time that SIRT1 is an important substrate of cysteine cathepsins. Its degradation by the cathepsins can thus represent a hitherto hidden mechanism linking cell stress with SIPS or apoptosis. Moreover, lysosomal membrane permeabilization and subversion of autophagy could also be associated with the accumulation of p62/SQSTM-1. It has recently been demonstrated that p62/SQSTM-1 accumulation not only is a marker of perturbed autophagic flux but may also affect cell viability by competing with the kelch-like ECH-associated protein 1 (Keap1) for a stress-response transcription factor Nrf2.[35] It has been shown that p62/SQSTM-1 binds to Keap1, the partner of Nrf2 assuring its degradation, and p62 accumulation stabilizes Nrf2 and hyperactivates its target genes. Although it has not been established whether Nrf2 hyperactivation may instigate cell senescence, one of the conditions leading to p62/SQSTM-1 accumulation, namely subverted autophagy, has been linked to cell aging.[5] Hence, it is possible, albeit not studied here, that the finding of subverted autophagy leading to p62/SQSTM-1 accumulation in and SIPS of stressed EPC can be at least in part attributed to the above Nrf2-Keap1–dependent mechanism.

Induction of autophagy is a part of an adaptive response to stress and is implicated in lifespan extension.[36–38] It has been proposed that disruption of autophagy induces cell senescence.[39] Our findings provide an integrative mechanism linking stress-induced lysosomal membrane permeabilization with cathepsin-mediated cleavage of SIRT1 and subverted autophagy in embryonic EPC, leading to their SIPS or apoptosis. Ebselen prevents SIRT1 depletion by improving lysosomal membrane integrity. This is not a trivial finding because, from the therapeutic standpoint, administration of ebselen, the clinical safety of which has been demonstrated, could represent a convenient attempt to pharmacologically manipulate the level of SIRT1. The proposed mechanism of SIRT1 depletion in stress has all of the attributes of being a paradigm of premature cell senescence: a broad range of stressors inducing it, the

commonality of lysosomal permeabilization, and universality of sirtuin action.

References

1. Erusalimsky JD, Kurz DJ: Endothelial cell senescence. Handb Exp Pharmacol 2006, 213–248
2. Patschan S, Chen J, Polotskaia A, Mendelev N, Cheng J, Patschan D, Goligorsky MS: Lipid mediators of autophagy in stress-induced premature senescence of endothelial cells. Am J Physiol Heart Circ Physiol 2008, 294:H1119–H1129
3. Patschan S, Chen J, Gealekman O, Krupincza K, Wang M, Shu L, Shayman JA, Goligorsky MS: Mapping mechanisms and charting the time course of premature cell senescence and apoptosis: lysosomal dysfunction and ganglioside accumulation in endothelial cells. Am J Physiol Renal Physiol 2008, 294:F100–F109
4. Rine J, Strathern JN, Hicks JB, Herskowitz I: A suppressor of mating-type locus mutations in Saccharomyces cerevisiae: evidence for and identification of cryptic mating-type loci. Genetics 1979, 93:877–901
5. Kennedy BK, Austriaco NR, Jr., Zhang J, Guarente L: Mutation in the silencing gene SIR4 can delay aging in S. cerevisiae. Cell 1995, 80:485–496
6. Haigis MC, Guarente LP: Mammalian sirtuins—emerging roles in physiology, aging, and calorie restriction. Genes Dev 2006, 20:2913–2921
7. Han MK, Song EK, Guo Y, Ou X, Mantel C, Broxmeyer HE: SIRT1 regulates apoptosis and Nanog expression in mouse embryonic stem cells by controlling p53 subcellular localization. Cell Stem Cell 2008, 2:241–251
8. Narala SR, Allsopp RC, Wells TB, Zhang G, Prasad P, Coussens MJ, Rossi DJ, Weissman IL, Vaziri H: SIRT1 acts as a nutrient-sensitive growth suppressor and its loss is associated with increased AMPK and telomerase activity. Mol Biol Cell 2008, 19:1210–1219
9. Mantel C, Broxmeyer HE: Sirtuin 1, stem cells, aging, and stem cell aging. Curr Opin Hematol 2008, 15:326–331
10. Lee IH, Cao L, Mostoslavsky R, Lombard DB, Liu J, Bruns NE, Tsokos M, Alt FW, Finkel T: A role for the NAD-dependent deacetylase Sirt1 in the regulation of autophagy. Proc Natl Acad Sci USA 2008, 105:3374–3379
11. Chen J, Li H, Addabbo F, Zhang F, Pelger E, Patschan D, Park HC, Kuo MC, Ni J, Gobe G, Chander PN, Nasjletti A, Goligorsky MS: Adoptive transfer of syngeneic bone marrow-derived cells in mice with obesity-induced diabetes: selenoorganic antioxidant ebselen restores stem cell competence. Am J Pathol 2009, 174:701–711
12. Chen J, Brodsky SV, Goligorsky DM, Hampel DJ, Li H, Gross SS, Goligorsky MS: Glycated collagen I induces premature senescence-like phenotypic changes in endothelial cells. Circ Res 2002, 90:1290–1298
13. Brodsky SV, Gealekman O, Chen J, Zhang F, Togashi N, Crabtree M, Gross SS, Nasjletti A, Goligorsky MS: Prevention and reversal of premature endothelial cell senescence and vasculopathy in obesity-induced diabetes by ebselen. Circ Res 2004, 94:377–384
14. Sharpless NE, DePinho RA: How stem cells age and why this makes us grow old. Nat Rev Mol Cell Biol 2007, 8:703–713
15. Hatzopoulos AK, Folkman J, Vasile E, Eiselen GK, Rosenberg RD: Isolation and characterization of endothelial progenitor cells from mouse embryos. Development 1998, 125:1457–1468
16. Kisanuki YY, Hammer RE, Miyazaki J, Williams SC, Richardson JA, Yanagisawa M: Tie2-Cre transgenic mice: a new model for endothelial cell-lineage analysis in vivo. Dev Biol 2001, 230:230–242
17. Dimri GP, Lee X, Basile G, Acosta M, Scott G, Roskelley C, Medrano EE, Linskens M, Rubelj I, Pereira-Smith O, Peacocke M, Campisi J: A biomarker that identifies senescent human cells in culture and in aging skin in vivo. Proc Natl Acad Sci USA 1995, 92:9363–9367
18. van der Loo B, Fenton MJ, Erusalimsky JD: Cytochemical detection of a senescence-associated beta-galactosidase in endothelial and smooth muscle cells from human and rabbit blood vessels. Exp Cell Res 1998, 241:309–315
19. Erwig LP, McPhilips KA, Wynes MW, Ivetic A, Ridley AJ, Henson PM: Differential regulation of phagosome maturation in macrophages and dendritic cells mediated by Rho GTPases and ezrin-radixin-moesin (ERM) proteins. Proc Natl Acad Sci USA 2006, 103:12825–12830
20. Rozman J, Stojan J, Kuhelj R, Turk V, Turk B: Autocatalytic processing of recombinant human procathepsin B is a bimolecular process. FEBS Lett 1999, 459:358–362
21. Bromme D, Nallaseth FS, Turk B: Production and activation of recombinant papain-like cysteine proteases. Methods 2004, 32:199–206
22. Mihelic M, Dobersek A, Guncar G, Turk D: Inhibitory fragment from the p41 form of invariant chain can regulate activity of cysteine cathepsins in antigen presentation. J Biol Chem 2008, 283:14453–14460
23. Turk B, Krizaj I, Kralj B, Dolenc I, Popovic T, Bieth JG, Turk V: Bovine stefin C, a new member of the stefin family. J Biol Chem 1993, 268:7323–7329
24. Cirman T, Oresic K, Mazovec GD, Turk V, Reed JC, Myers RM, Salvesen GS, Turk B: Selective disruption of lysosomes in HeLa cells triggers apoptosis mediated by cleavage of Bid by multiple papain-like lysosomal cathepsins. J Biol Chem 2004, 279:3578–3587
25. Lamark T, Kirkin V, Dikic I, Johansen T: NBR1 and p62 as cargo receptors for selective autophagy of ubiquitinated targets. Cell Cycle 2009, 8:1986–1990
26. Boya P, Kroemer G: Lysosomal membrane permeabilization in cell death. Oncogene 2008, 27:6434–6451
27. Petiot A, Ogier-Denis E, Blommaart EF, Meijer AJ, Codogno P: Distinct classes of phosphatidylinositol 3′-kinases are involved in signaling pathways that control macroautophagy in HT-29 cells. J Biol Chem 2000, 275:992–998
28. Tamai M, Matsumoto K, Omura S, Koyama I, Ozawa Y, Hanada K: In vitro and in vivo inhibition of cysteine proteinases by EST, a new analog of E-64. J Pharmacobiodyn 1986, 9:672–677
29. Roberg K, Ollinger K: Oxidative stress causes relocation of the lysosomal enzyme cathepsin D with ensuing apoptosis in neonatal rat cardiomyocytes. Am J Pathol 1998, 152:1151–1156
30. Yuan XM, Li W, Dalen H, Lotem J, Kama R, Sachs L, Brunk UT: Lysosomal destabilization in p53-induced apoptosis. Proc Natl Acad Sci USA 2002, 99:6286–6291
31. Repnik U, Turk B: Lysosomal-mitochondrial cross-talk during cell death. Mitochondrion 2010, 10:662–669
32. Terman A, Kurz T, Gustafsson B, Brunk UT: Lysosomal labilization. IUBMB Life 2006, 58:531–539
33. Addabbo F, Ratliff B, Park HC, Kuo MC, Ungvari Z, Csiszar A, Krasnikov B, Sodhi K, Zhang F, Nasjletti A, Goligorsky MS: The Krebs cycle and mitochondrial mass are early victims of endothelial dysfunction: proteomic approach. Am J Pathol 2009, 174:34–43
34. Kurz T, Eaton JW, Brunk UT: Redox activity within the lysosomal compartment: implications for aging and apoptosis. Antioxidants 13:511–523
35. Komatsu M, Kurokawa H, Waguri S, Taguchi K, Kobayashi A, Ichimura Y, Sou YS, Ueno I, Sakamoto A, Tong KI, Kim M, Nishito Y, Iemura S, Natsume T, Ueno T, Kominami E, Motohashi H, Tanaka K, Yamamoto M: The selective autophagy substrate p62 activates the stress responsive transcription factor Nrf2 through inactivation of Keap1. Nature 12:213–223
36. Terman A, Brunk UT: Autophagy in cardiac myocyte homeostasis, aging, and pathology. Cardiovasc Res 2005, 68:355–365
37. Rubinsztein DC, Gestwicki JE, Murphy LO, Klionsky DJ: Potential therapeutic applications of autophagy. Nat Rev Drug Discov 2007, 6:304–312
38. Harrison DE, Strong R, Sharp ZD, Nelson JF, Astle CM, Flurkey K, Nadon NL, Wilkinson JE, Frenkel K, Carter CS, Pahor M, Javors MA, Fernandez E, Miller RA: Rapamycin fed late in life extends lifespan in genetically heterogeneous mice. Nature 2009, 460:392–395
39. Levine B, Kroemer G: Autophagy in the pathogenesis of disease. Cell 2008, 132:27–42